Principles and Methodology to Explore Bidirectional Reflection Properties of Direct Radiative Remotely Sensed Image

Li Xianhua
(*Chengdu Institute of Mountain Disaster and Environment, Chinese Academy of Sciences and Ministry of Water Resources, Chengdu, 610041, China*)

Li Qi
(*RS & GIS Institute, Peking University, Beijing, 100087, China*)

Yu Genong
(*Chengdu Subcentre of Agricultural Remote Sensing, Chengdu, 610066, China*)

Lan Libo
(*Chengdu Institute of Mountain Disaster and Environment, Chinese Academy of Sciences and Ministry of Water Resources, Chengdu, 610041, China*)

Yang Wunian
(*Chengdu College of Science and Technology, Chengdu, 610023, China*)

Chi Tianhe
(*National Laboratory of Resources and Environment Information System, Institute of Geography, Chinese Academy of Sciences and State Planning Commission, Beijing, 100101, China*)

Huang Xueqiao
(*Chengdu Institute of Mountain Disaster and Environment, Chinese Academy of Sciences and Ministry of Water Resources, Chengdu, 610041, China*)

Abstract This paper describes the principles and methodology to express bidirectional reflection (BDR) properties of ground targets by using direct radiative remotely sensed image under the support of GIS. The principles and theoretical basis is that the difference of slope and its orientation changes the relative position of pixel ground, sun, and satellite remote sensor and results in the variety of solar direct radiance of similar pixels. The difference reflect the bidirectional reflectance. The bidirectional reflectance could be studied through the analysis of the difference and its relation with sun position and satellite position under the support of GIS, using satellite remotely sensed direct radiance digital images.

Key words Direct radiance, Remotely sensed image, Bidirectional reflectance

The significance of bidirectional reflectance study for multiangle visible light remote sensing is obvious. A new statistical search of bidirectional reflectance properties is the representation of bidirectional reflectance of typical targets using generated remotely sensed direct radiance images from satellite. The use of direct radiance images would lead the study of bidirectional reflectance into essence and have significant potentials in the applications.

1 GENERATION OF SATELLITE REMOTELY SENSED SOLAR DIRECT RADIANCE IMAGES

The procedure for the generation of solar direct radiance digital images: match satellite remotely sensed data, digital terrain model and solar irradiance fractions, calculate and divide the direct radiance fraction from remotely sensed data pixel by pixel by means of computer, sort the result by spectrum, and result in solar direct radiance digital image by simulating the conditions at the imaging time[1,2].

The direct radiance fraction of any non shadow pixel could be derived from equation (1).

$$D_{SKL} = D_{NKL} - D_{AKL} - D_{DKL} = D_{NKL} - D_{AKL} - D'_{DKL} \times G_{KL} \quad (1)$$

where, D_{NKL} and D_{AKL} is original remotely sensed value and atmospheric distant radiation of any pixel re-

spectively; D_{DKL} is the remotely sensed scattering radiance fraction of the pixel resulted from skylight. Assuming that scattering radiance of any pixel at horizontal ground surface be derived using equation (2).

$$D'_{DKL} = D_{DKL}/G_{KL} \quad (2)$$

where, G_{KL} is skylight irradiance on any pixel, checked out on related digital terrain map[1].

The remotely sensed direct radiance of any pixel in shadow is zero. To derive the direct radiance image, it is provided that the direct radiance of a shadow pixel is its remotely sensed direct radiance when it is not in shadow[1].

$$D_{Sij} = D'_{Sij}F_{ij} = D_{Dij} \times F_{ij}/L_{ij} \times G_{ij} \quad (3)$$

$$L_{ij} = D'_{Dij}/D'_{Sij} \quad (4)$$

$$W_{ij} = A_{ij} - AL_{ij} \quad (5)$$

$$F_{ij} = 1 - tg\alpha_{ij}ctg\theta_{ij}cos\omega_{ij} \quad (6)$$

where, D_{Sij} is the remotely sensed direct radiance of a pixel on a horizontal surface; α_{ij} and θ_{ij} are slope degree of the ground surface and the altangle of sun to the horizontal ground surface; A_{ij} and AL_{ij} are the slope orientation of pixel and the sun azimuth.

2 SUN ALTANGLE AND AZIMUTH AT A PIXEL

The sun altangle and azimuth of any pixel on a satellite remotely sensed image, at any given imagine moment, depends upon the geographical location of the pixel and the ground slope and its orientation, except for those marked out by the legend, like satellite nadir location, sun altangle and azimuth at nadir, pixel size, etc.

Determination of sun altangle and azimuth at any pixel on a horizontal ground surface

The imaging time, satellite nadir geographical latitude and longitude, and sun altangle and azimuth at nadir are given by the legend of a satellite remotely sensed image. Any given pixel, however, differs on sun altangle and azimuth on a horizontal surface, due to the variety of its nadir position[3]. Fig. 1(a) shows the case, where P_0 is the satellite nadir point, P_{ij} is any given pixel, θ_{ij} is the sun altangle, and A is the sun azimuth.

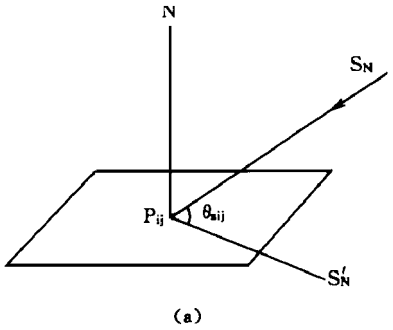

(a)

Fig. 1(a) Sun altangle and azimuth of any pixel at a horizontal ground surface

The sun altangle of any given pixel Pij at a horizontal surface can be derived from equation (7).

$$\theta_{ij} = \arcsin(\sin\phi_{ij}\sin\delta_{ij} + \cos\phi_{ij}\cos\delta\cos t_{ij}) \quad (7)$$

where, sun latitude

$$\delta = \arcsin(\sin\theta_0\sin\phi_0 - \cos\theta_0\cos\phi_0\cos A_0) \quad (8)$$

time angle of any given pixel

$$t_{ij} = t_0 + \Delta\lambda_{ij} \quad (9)$$

$$\Delta\lambda_{ij} = \lambda_{ij} - \lambda_0 \quad (10)$$

$$t_0 = \arcsin(\cos\theta_0 \times \sin A_0/\cos\delta) \quad (11)$$

The sun azimuth of pixel P_{ij}:

$$AS_{ij} = \arcsin[(\sin\theta_{ij}\sin\phi_{ij} - \sin\delta) - \cos\theta_{ij}\cos\phi_{ij}] \quad (12)$$

where, ϕ_{ij} and λ_{ij} are latitude and longitude of the pixel; θ_0, A_0, λ_0, ϕ_0, and t_0 are sun altangle, sun azimuth, latitude/longitude and time angle of the nadir point on a horizontal ground.

Determination of sun altangle and azimuth at any pixel on a slope surface

The difference of slope degree and orientation varies sun altangle and azimuth of pixel on slopes because of the relative geometrical orientation. See Fig. 1(b).

In Fig. 1(b), P_{ij} is the pixel; α_{ij} and AL_{ij} are slope angle and slope orientation of slope ABCD, A′B′CD is the projection of surface ABCD on to horizontal surface, θ_{sij} is the sun altangle of A′B′CD; θ'_{sij} is the sun altangle of slope surface P_{ij}, A'_{sij} is its sun azimuth.

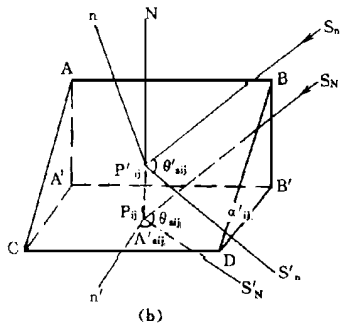

Fig. 1(b) Sun altangle and azimuth of any pixel at a slope surface

$$A'_{sij} = AS_{ij} - AL_{ij} \quad (13)$$

$$\theta'_{sij} = \cos\theta_{ij}\cos\alpha_{ij} + \sin\theta_{sij}\sin\alpha_{ij}\cos A'_{sij} = \arccos(\cos\theta_{sij}\cos\alpha_{ij} + \sin\theta_{sij}\sin\alpha_{ij}\cos A'_{sij}) \quad (14)$$

Examples for calculating sun altanlge and azimuth of any Pixel

Xichang MSS scene, imaged on Greenwich Mean Time 03:11:10 January 3, 1974, was used as an example to calculate nadir position and sun altangle and azimuth of four corner pixel on slope and/or plain[3]. See Table 1.

Table 1 Nadir position and sun altangle and azimuth of four corner pixel on slope and/or plain

Image type	Time(local)	Pixel	λ	ϕ	α	AL	θ_s	AS	A'_s	θ'_s
MSS	3.186 January 3,1974	Nadir	111.82	27.28	6	−72	31	145	217	36.0
	Latitude: −22.832	0,0	101.86	27.90	26	112.3	30.0	144.3	32	15.3
	Nadir time angle: −32.242	3240,0	102.47	28.30	11	−71.1	30.5	145.9	217	39.8
		0,2340	101.16	26.27	9	−17.9	31.5	144.1	162	40.2
		3240,2340	101.82	27.28	7	−158.4	32.0	145.7	304	28.6

Calculation for the pixel at nadir:

$$A_{s0} = AS_{ij} - AL_{ij} = 145 + 72 = 217 \quad (15)$$

$$\theta'_s = \arccos(\cos\theta_{s0}\cos\alpha_0 + \sin\theta_{s0}\sin\alpha_0\cos A_{s0}) = \arccos(\cos 31\cos 6 + \sin 31\sin 6\cos 217) = 36.0 \quad (16)$$

See Table 1 for results of other four point. The variety of sun altangle and azimuth of every pixel on remotely sensed satellite image relates to its located latitude[3]. The higher the latitude is, the more drastic the change is. The change, however, is little, between 0°—2° for low to middle latitude.

The change of sun altangle and azimuth of slope pixel relies much upon slope degree and orientation, between 0°—90° for sun altangle and 0°—360° for sun azimuth.

3 CALCULATION OF SATELLITE ALTANGLE AND AZIMUTH

The calculation of satellite altangle and azimuth for each pixel on satellite remotely sensed image is similar to that for sun. Firstly, calculate satellite altangle and azimuth providing a horizontal plain, and then, calculate satellite altangle and azimuth on slope using slope degree and orientation of pixel surface.

Satellite altangle and azimuth for pixels on horizontal plain

In Fig. 2(a), E is the place where satellite locate, P_0 is the nadir of satellite, i.e. (i_0, j_0), and P_{ij} is the pixel at column i and row j in a satellite remotely sensed image.

The distance between P and satellite nadir:

$$E_0P = [(i - i_0)^2 S_y^2 + (j - j_0)^2 S_x^2]^{0.5} \quad (17)$$

Satellite altitude:

$$h_0 = h_e + e1e = EE_0 \quad (18)$$

where, S_y and S_x are width and length of pixel plot on the ground, H_e is satellite altitude and e1e is the modification value. All these values, i_0 and j_0 depends upon satellite type.

Providing that the original is at the nadir of

satellite, the satellite altangle at pixel P on a horizontal plain can be calculated out using equation (19).

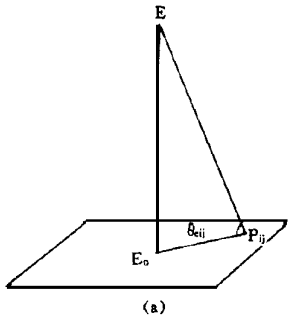

Fig. 2(a) Satellite altangle and azimuth on a horizontal ground in a remotely sensed image

$$\theta_{eij} = \mathrm{arctg}(EE_0/E_0P) = \mathrm{arctg}[(H_e - e_1e)/[(i')^2 \times S_y^2 + (j')^2 \times S_x^2]^{0.5}] \quad (19)$$

Satellite azimuth at pixel P on a horizontal plain can be derived using formula (20).

$$A_{ei,j} = \mathrm{arctg}[i' \times S_y / j' \times S_x] + H_0 \quad (20)$$

$$H_0 = H_s + H_e \quad (21)$$

$$i' = i_{ij} + I_0 \quad (22)$$

$$j' = j - j_0 \quad (23)$$

where, H_s is the standard azimuth of satellite; H_e is the azimuth change due to earth evolution; H_0 is satellite azimuth.

Satellite altangle and azimuth for pixels on slope

Given satellite altangle and azimuth of pixel on a horizontal plain, the methodology to calculate satellite altangle and azimuth of pixel on a slope, using slope degree and orientation derived from DTM, is similar to that for sun. See Fig. 2(b).

In Fig. 2(b), P_{ij} is pixel on slope ABCD; AL_{ij} is the slope orientation and θ_{eij} is slope angle. Corresponded to horizontal plain A'B'CD, the satellite altangle is θ_{eij} and the satellite azimuth is AE_{ij}; α_0 is slope angle of satellite nadir point P_{ij} and AL_{ij} is its orientation. Satellite azimuth on slope is calculated using equation (24).

$$A'_{eij} = AE_{ij} - AL_{ij} \quad (24)$$

Satellite altangle on slope can be derived from equation (25).

$$\theta'_{eij} = \arccos(\cos\theta_{eij}\cos\alpha_{ij} + \sin\theta_{eij}\sin\alpha_{ij}\cos A'_{eij}) \quad (25)$$

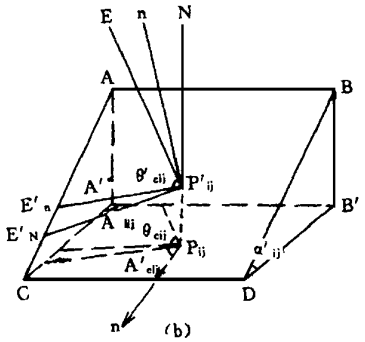

Fig. 2(b) Satellite altangle and azimuth on a slope in a remotely sensed image

Examples

Using left top corner of Xichang scene of MSS as an example, calculate the satellite altangle and azimuth.

$$\theta_{e0,0} = \mathrm{arctg}(ee_0/EP_{ij}) \approx \mathrm{arctg}[(H_e + e_1e)/[(i - i_0)^2 S_x^2 + (j - j_0)^2 S_y^2]^{0.5}] \approx \mathrm{arctg}[950000/[1620^2 \times 60^2 + 1170^2 \times 80^2]^{0.5}] = 80.9 \quad (26)$$

$$AE_{0,0} = \mathrm{arctg}(j' s_y)/(i' s_x) + H_0 = \mathrm{arctg}(1170 \times 80)/(-1620 \times 60) + 4.85 = \mathrm{arctg}(-0.9630) \approx 313.9 \quad (27)$$

$$\theta_{e0,0} = \arccos(\cos\theta_{e0,0}\cos\alpha_{0,0} + \sin\theta_{e0,0}\sin\alpha_{0,0}\cos A'_{e0,0}) = \arccos(\cos 89.2 \cos 21 + \sin 89.2 \sin 21 \cos(325.13)) \approx \arccos(0.307) \approx 72.12 \quad (28)$$

The results for satellite altangle and azimuth of other four points can be seen in Table 2.

The following could be found out from Table 2.

Table 2 Satellite altangle and azimuth of four corner pixels and nadir pixel on Xichang Landsat MSS scene

Pixel	AL	α	AE	θ_e	A_e'	θ_e'
Nadir	−72.0	6	0.0	90.0	72.0	84
0,0	112.3	26	313.9	80.9	201.6	75
3240,0	−71.1	11	43.9	80.9	115.0	86
0,2340	17.9	9	226.1	80.9	208.2	89
3240,2340	−158.4	71	33.9	80.9	292.2	78

(1) The satellite azimuth changes within 0°—360° when the relative position between image pixel and satellite nadir point differs for pixels on a horizontal plain, while the satellite altangle changes within 81°—90°.

(2) For pixels on a slope, the satellite altangle changes within 0°—90° and the satellite azimuth changes within 0°—360° while the pixel slope orientation and angle varies.

The satellite altangle and azimuth in any direction, for natural ground surface, is possible due to the above reasons.

4 BIDIRECTIONAL REFLECTION OF GROUND TARGETS ON A REMOTELY SENSED DIRECT RADIANCE IMAGE

The difference of slope angle and orientation cause not only the varieties of reflection direction but also the diversities of sun irradiation direction[4], for a satellite remotely sensed direct radiance image is the result of sun direct irradiance. This makes the study of bidirectional reflectance possible on a remotely sensed direct radiance image.

Orientation parameters of bidirectional reflection of pixel targets on a slope

Fig. 3(a) shows the geometrical parameters related to bidirectional reflection of pixel P on a plain, where PN is a vertical line to a horizontal plain, S and E are sun and satellite respectively, PS′ is the intersection line of sun irradiance surface and horizontal surface passing P, then sun altangle of P is θ_{SP} = ∠SPS′. Slope angle of the pixel is zero and then sun irradiance azimuth of P is $\Phi_{TP} = AS_p$. E′ is satellite nadir, E is satellite and then satellite altangle of pixel P on a plain is $\theta_{ep} = AE_p$.

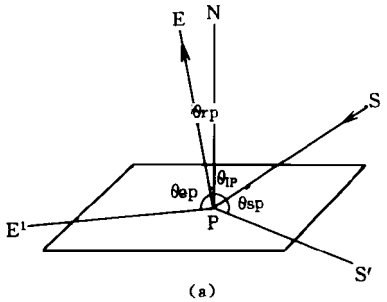

Fig. 3(a) Geometrical parameters for bidirectional reflection on a horizontal ground

Fig. 3(b) shows that on a slope. PN is the normal line of slope with slope orientation AL_p and angle α_p, the intersection line of sun irradiance surface passing P with slope is PO and that with horizontal surface is $P_s'O$, and

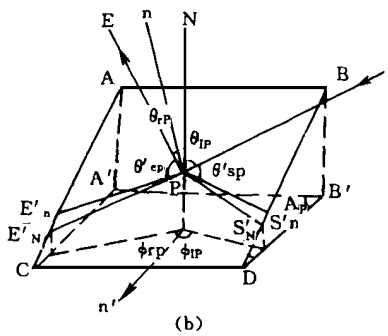

Fig. 3(b) Geometrical parameters for bidirectional reflection on a slope

then horizontal sun altangle is $\theta_{SP} = \angle SP_sO$. The angle between sunlight irradiance surface and slope is $A_{sp}' = AS_p - AL_p$, the intersection line between the surface where the slope normal line PN passing P and PS locates and the slope is PS′, and then sun altangle

on slope is $\theta'_{sp} = \angle SPS$. The surface EPN intersect slope at PP′, then slope satellite altangle is $\theta'_{ep} = \angle EPE'$ and slope satellite azimuth is $A'_{ep} = AE_p - AL_p$.

N is the zenith. The sunlight incident azimuth on a slope:

$$\phi_{IP} = \angle S'PN = A'_{IP} = AS_p - AL_p \quad (29)$$

The sunlight incident angle on a slope:

$$\theta_{IP} = \angle SPP' = 90^\circ - \theta'_{SP} = 90^\circ - \arccos(\cos\theta_{SP}\cos\alpha_P + \sin\theta_{SP}\cos\alpha_P\cos\phi_{IP}) \quad (30)$$

The sun direct reflection azimuth on a slope:

$$\phi_{IP} = \Delta\alpha_{IP} = A_{ep} - A_{ip} \quad (31)$$

The sun direct reflection angle on a slope:

$$\theta_{IP} = \angle NPE = 90^\circ - \theta'_{ep} = 90^\circ - \arccos(\cos\theta_{ep}\cos\alpha_P + \sin\theta_{ep}\sin\alpha_P\cos\phi_{IP}) \quad (32)$$

Sunlight direct irradiance of pixel on a slope

The undulation of ground surface affects the direct irradiance of pixel on a slope.

θ_{KL} is the sun altangle of slope pixel ρ_{KL}, α_{KL} is slope angle, and ϕ_{IKL} is the included angle between sunlight incident direction and slope orientation.

To simplify the calculation, use the penetrability τ_0 of homogeneous atmosphere. E_{s0} is the sun spectral irradiance vertical to sunlight. When the sun altangle is θ_{KL}, the sun spectral irradiance on a horizontal surface:

$$E'_{KL} = E_{s0} \times \cos(90^\circ - \theta_{KL}) \times \tau_0^{\sec(90-\theta_{KL})} = E_{s0} \times \sin\theta_{KL} \times \tau_0^{\csc\theta_{KL}} \quad (33)$$

Slope sun spectral irradiance[2]:

$$E_{SKL} = E'_{SKL}(1 - \mathrm{tg}\alpha_{KL}\mathrm{ctg}\theta_{KL}\cos\phi_{IKL}) = E_{s0}\sin\theta_{KL}(1 - \mathrm{tg}\alpha_{KL}\mathrm{ctg}\theta_{KL}\cos\varphi_{IKL})\tau_0^{\csc\theta_{KL}} \quad (34)$$

Calculation of slope pixel ground reflectance on a remotely sensed direct radiance image

The four band remote sensing value of slope pixel KL on a remotely sensed direct radiance image:

$$D_{SKL} = KE_{SKL} \times \tau_0 \times \rho_{KL}/\pi \quad (35)$$

The reflectance at the slope pixel:

$$\rho_{KL} = D_{SKL} \times \pi/K \times \tau_0 \times E_{SKL} \quad (36)$$

Substitute equation (34) into (36), then

$$\rho_{KL} = D_{SKL} \times \pi/K \times \tau_0 \times E_{s0}\sin\theta_{KL}(1 - \mathrm{tg}\alpha_{KL}\mathrm{ctg}\theta_{KL}\cos\phi_{IKL})\tau_0^{\csc\theta_{KL}}$$

Given constant $C = \pi/K \times E_{s0} \times \tau_0$, then

$$\rho_{KL} = D_{SKL} \times C \times \sin\theta_{KL}(1 - \mathrm{tg}\alpha_{KL}\mathrm{ctg}\alpha_{KL}\cos\phi_{IKL}) \quad (38)$$

where, τ_0 is atmospheric spectral vertical penetrability, and K is the inlaid transformation coefficients of MSS system.

Bidirectional reflectance on a remotely sensed direct radiance image

ρ_{KL} is pixel, ϕ_{KL} is the sunlight incident azimuth on a slope, and the incident angle is θ_{IKL}. When the reflection azimuth is ϕ_{IKL} and the reflection angle is θ_{IKL}, the reflectance

$$\rho_{KL} = \rho_R(\theta_{IKL}, \phi_{IKL}, \theta_{\tau KL}, \phi_{\tau KL}) \quad (39)$$

where,

$$\theta_{IKL} = 90^\circ - \theta_{SKL} = 90^\circ - \arccos(\cos\theta_{SKL}\cos\alpha_{KL} + \sin\theta_{SKL}\sin\alpha_{KL}\cos\phi_{IKL}) \quad (40)$$

$$\theta_{\tau KL} = 90^\circ - \theta_{eKL} = 90^\circ - \arccos(\cos\theta_{eKL}\cos\alpha_{KL} + \sin\theta_{eKL}\sin\alpha_{KL}\cos\phi_{eKL}) \quad (41)$$

$$\phi_{IKL} = AS_{KL} - AL_{KL} \quad (42)$$

$$\phi_{\tau KL} = AE_{KL} - AL_{KL} \quad (43)$$

$$C = \pi/K \times E_{s0} \times \tau_0 \quad (44)$$

$$0^\circ < \alpha_{KL} < 90^\circ;\ 0^\circ < \theta_{SKL} < 90^\circ;\ 0^\circ < AS_{KL} < 360^\circ;\ 0^\circ < AL_{KL} < 360^\circ$$

$$\rho_R(\theta_{IKL}, \phi_{IKL}, \theta_{\tau KL}, \phi_{\tau KL}) = D_{SKL} \times C \times \sin\theta_{KL}(1 - \mathrm{tg}\alpha_{KL}\mathrm{ctg}\theta_{KL}\cos\phi_{IKL}) \quad (45)$$

Given atmospheric penetrability and sun spectral irradiance E_s at the vertical direction to sunlight, use equation (32) to calculate the reflectance of pixel on slopes from a remotely sensed direct radiance image. Here shows the calculation of top left corner point of Xichang MSS scene as an example.

Calculation of direct radiance of band 4[5]:

$$D_{s0,0} = 9,\ K = 25.93,\ E_{s0} \approx 177.03,\ t_0 = 0.55 \quad (46)$$

$$C = \pi/25.93 \times 0.55 \times 117.03 = 0.00188 \quad (47)$$

$$\rho_{0,0} = D_{s0,0} \times C/\sin\theta_{s0,0} \times (1 - \mathrm{tg}\alpha_{0,0}\mathrm{ctg}\theta_{s0,0}\cos\phi_{i0,0}) \times t_0^{\csc\theta_{s0,0}}$$

$=9\times0.0001250\times\sin30.0(1-\mathrm{tg}26\mathrm{ctg}30.0\times\cos32)\times0.55^{\sec\theta_{s0,0}}$

$=9/(530.5\times0.316\times0.1512)=0.35$

See Table 3 for the results for other four points.

Table 3 Slope reflectance of pixels at satellite nadir and four corner

Pixels	D_s	F	$1/C$	$\sin\theta\times\tau^m$	ρ
Nadir	51	1.1397	530.5	0.1613	0.52
0,0	9	0.316	530.5	0.1512	0.35
3240,0	26	1.258	530.5	0.1561	0.24
0,2340	24	1.251	530.5	0.1162	0.31
3240,2340	32	0.8901	530.5	0.1714	0.40

Ground bidirectional reflectance on a remotely sensed direct radiance image

The typical targets, like grassland, ice and snow, dunes, and crops, distributes extensively and largely on a diversities of land with different geomorphological features[4]. The pixel slope azimuth ranges from 0° to 360°, and its angle shows from 0° to 90°. Considering the similarity of the same ground targets, the geometrical parameters for bidirectional reflection on slope could be described in other words, i.e., providing sun and satellite is constant, a pixel, with a changing azimuth between 0°to 360° and a varying slope angle between 0°to 90°, diversifies its geometrical parameters of bidirectional reflection and reflectance. This means that the change of geometrical parameters (θ_i, θ_τ, ϕ_i, ϕ_τ) of ground bidirectional reflection at every pixel in a scene with diversified relief features, sunlight incident irradiance and satellite reflectance absorption equals to that at every pixel whose slope normal line changes in a semi-sphere. The total reflectance of many pixels which are selected to include the typical ground target on different slopes from a remotely sensed direct radiance image, therefore, represents the general bidirectional reflection properties of this type of ground target.

Given the ground target at four corner and nadir is grassland in a scene, Table 4 shows the bidirectional reflectance statistics of grassland.

Table 4 Reflectance of pixel at four corner and nadir in a satellite remotely sensed image

Pixel	Type	θ_i	ϕ_i	θ_τ	ϕ_τ	ρ_τ	Band
Nadir	Grassland	54	217	2	72	0.445	4
0,0	Grassland	75	32	15	206	0.023	4
3240,0	Grassland	51	217	2	122	0.261	4
0,2340	Grassland	50	162	1	167	0.322	4
3240,2340	Grassland	61	304	14	20	0.220	4

Calculate the geometrical parameters and the reflectance for every slope pixel of typical targets pixel by pixel and band by band using computer. The results is up to 10^6. Process the resulted data by means of mathematical statistics, necessary interpolation and induction, and tiding and set up a bidirectional reflection data base for typical targets. See Table 5 for the data format.

Table 5 Data format of the bidirectional reflection data base for typical targets

Typical data	Bands 4—7	sun azimuth $360^\circ:\Delta\phi_i-5^\circ$	Sun incident angle $90^\circ:\Delta\theta_i-5^\circ$	Reflection azimuth $360^\circ:\Delta\phi_\tau-5^\circ$	Reflective angle $90^\circ:\Delta\theta_\tau-5^\circ$	Reflectivity

It is ease, by using this data base, to study the distribution of bidirectional reflection of typical targets at any datum face on a satellite remotely sensed image and analyze the bidirectional reflection distribution of a target with a definite sunlight incident azimuth, incident angle and reflection angle but indefinite reflection azimuth ranging from 0°to 360°. This also meets the requirements to study the bidirectional reflection principles in terms of three dimensions, multilevel and all aspects.

5 QUESTIONS AND CONCLUSIONS

The combination of remotely sensed direct radiance image, clear of atmospheric and skylight inference, and digital terrain model provides a new means and a new material to study bidirectional reflection properties of typical targets in natural environment.

Some principles and methodology to study bidirectional reflectance of typical ground targets on a satellite remotely sensed image by using a derived remotely sensed direct radiance image is discussed although the study is not yet fully carried through. Some questions are expected to be clear with the ongoing project, like the following.

(1) There is no target 's bidirectional reflectance completed yet.

(2) The accuracy of method can not be determined objectively since there no enough comparison data from field.

(3) The concordance between pixel incident azimuth and slope pixel sunlight azimuth need to be proved precisely.

The following conclusions could be reached even though there are the above doubts.

The satellite remotely sensed data, in precise words, are products of multiangle remote sensing, especially those for mountainous areas[6].

It is possible to calculate slope sun altangle and azimuth and slope satellite altangle and azimuth of every pixel by matching satellite remotely sensed image and digital terrain model, and then derive the geometrical parameters of slope bidirectional reflectance at every pixel.

The slope direct light reflectivity can be derived by using a remotely sensed direct radiance image and matching digital terrain model, which is resulted from the incident angle and incident azimuth of sunlight onto a slope at every pixel and the reflective angle and reflective azimuth of satellite to the slope.

Some simple statistic rules, about the reflectance of targets with different reflective azimuth and reflective angle but unified in light incident angle and incident azimuth, can be studied through the calculation and statistical analysis of sunlight incident azimuth and incident angle, reflective azimuth and reflective angle, and reflectance of ground targets on slopes at over thousands of pixels, using computer. It is a new method to study bidirectional reflectance of ground targets all inclusively and thoroughly within a three dimension space, which is of significance for the fully understanding of principles and mechanism of bidirectional reflection and multiangle remote sensing.

REFERENCE

[1] Li Xianhua, L. Lan, X. Huang *et al*. Computer formation about Satellite Remotely Sensed Images of Each Branch of Natural Solar Radiation. *Remote Sensing of Environment, China*, 1995, **10**(3):217—223.

[2] Li Xianhua. A Radiometric Correction of Relief Disturbances in the Remote Sensed Data. *Acta Geodetica et Cartographica Sinica*. 1986, **15**(2):102—109.

[3] Li Xianhua, X. Huang, T. Chi *et al*. Computation of Solar Elevations and Azimuths at Pixels of Satellite Image. In Chinese with English abstract. *Acta Ceodetica et Cartographica Sinica*. 1993, **22**(2):149-154.

[4] Tong Qingxi *et al*. Spectra and Analysis of Typical Earth Objects of China. Science Press. 1990.

[5] Chen Jicheng. System Approach in Remote Sensing Information Research. 1986.

[6] Yan S., Tong Q. Earth Resources Technology Satellite. 1980.

AUTHOR

Li Xianhua was born on January 29, 1949, and obtained M. S. & BSc. at Dept. of RS, Zhejiang University. Now he is a researcher in Chengdu Institute of Mountain Disaster and Environment, Chinese Academy of Science. His interests are remote sensing and GIS. He has more than 30 publications.

基于直射辐射遥感图象的地物双向反射特性研究

李先华

(中国科学院 水 利 部成都山地灾害与环境研究所，成都，610041，中国)

李 琦

(北京大学 RS 与 GIS 研究所，北京，100087，中国)

喻歌农

(四川省农业科学院农业遥感中心，成都，610066，中国)

兰立波

(中国科学院 水 利 部成都山地灾害与环境研究所，成都，610041，中国)

杨武年

(成都理工学院，成都，100087，中国)

池天河

(中国科学院 国 家 计 委 地理研究所，资源与环境信息系统国家重点实验室，北京，100101，中国)

黄雪樵

(中国科学院 水 利 部 成都山地灾害与环境研究所，成都，610041，中国)

摘 要 该文讨论了一种在 GIS 支持下利用直射辐射遥感图象研究地物双向反射特性的原理和方法。其主要依据是象元地面的坡度和坡向的不同，同时改变了象元地面与太阳之间、象元地面与卫星传感器之间的相对位置，并且造成了同类象元太阳直射辐射遥感分量的差异。而正是这种差异体现了该类地物双向反射特性。在 GIS 的支持下利用卫星直射辐射遥感数字图象，研究卫片象元同类地物的这种差异的规律以及它们与对应坡面上的太阳位置、卫星位置的关系，便可进行该类地物的双向反射特性研究。

关键词 直射辐射，遥感图象，双向反射特性